

Semiconductor plasmonic crystals: active control of THz extinction

This content has been downloaded from IOPscience. Please scroll down to see the full text.

2013 Semicond. Sci. Technol. 28 124003

(<http://iopscience.iop.org/0268-1242/28/12/124003>)

View [the table of contents for this issue](#), or go to the [journal homepage](#) for more

Download details:

IP Address: 194.171.111.64

This content was downloaded on 11/12/2013 at 07:44

Please note that [terms and conditions apply](#).

INVITED ARTICLE

Semiconductor plasmonic crystals: active control of THz extinction

M C Schaafsma¹ and J Gómez Rivas^{1,2}¹ Center for Nanophotonics, FOM Institute AMOLF, Science Park 104, 1098 XG, Amsterdam, The Netherlands² COBRA Research Institute, Eindhoven University of Technology, P.O. Box 513, 5600 MB Eindhoven, The NetherlandsE-mail: m.schaafsma@amolf.nl

Received 3 July 2013, in final form 18 August 2013

Published 13 November 2013

Online at stacks.iop.org/SST/28/124003

Abstract

We investigate theoretically the enhanced THz extinction by periodic arrays of semiconductor particles. Scattering particles of doped semiconductors can sustain localized surface plasmon polaritons, which can be diffractively coupled giving rise to surface lattice resonances. These resonances are characterized by a large extinction and narrow bandwidth, which can be tuned by controlling the charge carrier density in the semiconductor. The underlying mechanism leading to this tuneability is explained using the coupled dipole approximation and considering GaAs as the semiconductor. The enhanced THz extinction in arrays of GaAs particles could be tuned in a wide range by optical pumping of charge carriers.

(Some figures may appear in colour only in the online journal)

1. Introduction

The field of surface plasmon polariton optics (plasmonics) has attracted increased interest over the last decade. This interest has been motivated by the resonant response of metallic structures, which leads to an enhanced optical response and to large local field enhancements in subwavelength volumes [1, 2]. In their pioneering work, Ebbesen and co-workers demonstrated the enhanced optical transmission through metallic thin films perforated with subwavelength holes [3]. This enhanced transmission was explained in terms of the grating assisted excitation of surface plasmon polaritons (SPPs). Enhanced transmission of low-frequency electromagnetic radiation was demonstrated in the THz range by Gómez Rivas and co-workers [4]. An important characteristic of this work is that the perforated thin film was made of doped silicon. Doped semiconductors have a metallic behavior at THz frequencies, which enables the excitation of SPPs. The characteristics of SPPs can be tuned by controlling the carrier concentration in the semiconductor, which can be achieved by doping [5] or, actively, with magnetic fields [6, 7], or by thermal- [8–10], photo-excitation [11–15] or electrical injection of charge carriers [16]. Complementary to hole arrays are arrays of metallic particles exhibiting very narrow

bands with extraordinary extinction [17–19]. These bands, known as surface lattice resonances (SLRs) are the result of the enhanced radiative coupling of localized SPPs through Rayleigh anomalies (RA) (diffracted orders in the plane of the array) [20]. So far, SLRs have been mostly investigated at optical and near IR frequencies [21–26]. The few works on diffractive coupling of localized resonances at THz frequencies have been done on metallic structures [27–30], with the exception of [31] where arrays of Si resonators have been considered. However, in that reference no connection with SLRs was made.

In this manuscript we investigate theoretically the excitation of SLRs in 1D arrays of GaAs particles at THz frequencies. GaAs is a high mobility semiconductor with an energy bandgap of 1.43 eV ($\lambda_{\text{gap}} = 867$ nm), which allows for the optical excitation of free charge carriers using near IR wavelengths. This characteristic enables actively tuning the THz extinction of the SLRs in the arrays at defined wavelengths over a wide range as opposed to most metals which behave as nearly perfect electric conductors at THz frequencies and cannot be actively tuned. The large tuneability of the extinction makes SLRs in semiconductors interesting for THz modulation. The manuscript is organized as follows: the dielectric properties of GaAs in the THz regime as calculated

with the Drude model are described as a function of both frequency and carrier concentration in section 2.1. Using these material properties, we discuss localized surface plasmons (LSPs) in GaAs ellipsoids in section 2.2. The coupled dipole approximation is described in section 3.1, while the active control of the extinction in arrays of GaAs scatterers is discussed in section 3.2.

2. THz plasmonic particles

2.1. Drude model for GaAs

Semiconductors are excellent candidates for THz plasmonics. Doped semiconductors have a skin depth sufficiently large to allow for extensive penetration of THz radiation into the material, and a plasma frequency in the range of tens of THz. Their permittivity depends on the concentration of charge carriers, which can be controlled either by chemical doping, or actively by thermal- or photo-excitation of carriers, or by electrical injection. The frequency dependent complex permittivity ϵ resulting from the Drude model of free charge carriers is given by

$$\epsilon(\omega) = \epsilon_\infty + \frac{i\sigma}{\omega\epsilon_0}, \quad (1)$$

with ϵ_∞ the high frequency limit for the permittivity, $\omega = 2\pi\nu$ is the angular frequency, ϵ_0 the vacuum permittivity and σ the complex conductivity given by [32]

$$\sigma = \frac{10^6 N e^2 \tau / m}{1 - i\omega\tau}, \quad (2)$$

where N is the charge carrier density in cm^{-3} , e the fundamental charge, τ the carrier momentum relaxation time or the average time between charge carrier scattering events and m the charge effective mass. The momentum relaxation time depends on the carrier mobility, μ_m , and its effective mass through the relation $\tau = m\mu_m/e$, where μ_m depends on the charge carrier density. For n-doped GaAs, μ_m is approximated by the empirical relation [33]

$$\mu_m = \frac{0.94}{1.0 + (10^{-17}N)^{0.5}}. \quad (3)$$

Defining the plasma frequency as $\omega_p^2 = Ne^2/m\epsilon_0$, the complex permittivity can be written as

$$\epsilon = \epsilon_\infty - \frac{\omega_p^2}{\tau^{-2} + \omega^2} \left(\frac{1}{i\omega\tau} + 1 \right), \quad (4)$$

in which, for the calculations presented below, we use the following material properties for GaAs, $m = 1.39 \times 10^{-32}$ kg and $\epsilon_\infty = 10.89$ [34].

The permittivity of GaAs at THz frequencies is shown in figure 1 for various carrier concentrations, namely, $2 \times 10^{17} \text{ cm}^{-3}$ (blue curves), $5 \times 10^{17} \text{ cm}^{-3}$ (green curves), and 10^{19} cm^{-3} (red curves). The permittivity can be tuned over a significant range of values by changing the carrier concentration. Changes in the carrier concentration of the order of 10^{19} cm^{-3} can be reached by optical pumping [35]. Increasing the carrier concentration increases the plasma frequency, giving to the material a more metallic behavior, i.e., the magnitude of the real component of the permittivity increases, but also increases the imaginary component associated with the Ohmic losses in the semiconductor.

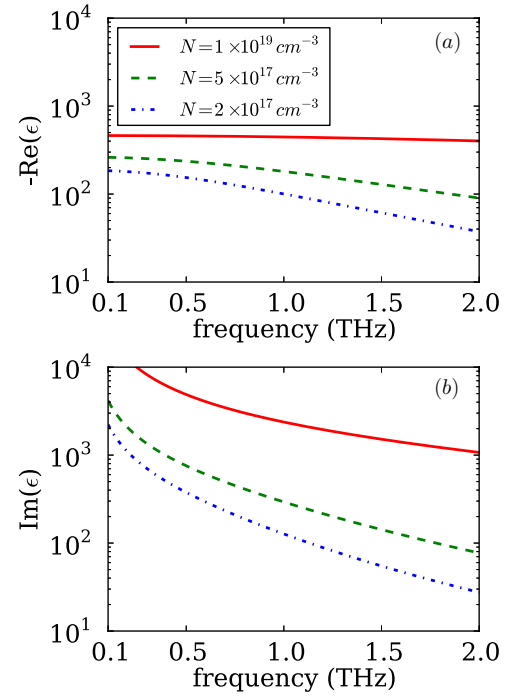


Figure 1. Minus real (a) and imaginary (b) component of the permittivity of GaAs for various carrier concentrations, as calculated with the Drude model of free charge carriers.

2.2. GaAs localized surface plasmons

The extinction properties of a scattering particle are given by its polarizability tensor, which depends on the shape and size of the particle, and the permittivity of the materials forming the particle and its surrounding. The principal components of the static polarizability of an ellipsoidal particle in a dielectric and homogeneous medium is given by [36]

$$\alpha_m^{\text{static}} = V \frac{(\epsilon_p - \epsilon_s)}{(3(\epsilon_p - \epsilon_s) \cdot L_m + 3\epsilon_s)}, \quad (5)$$

where $m = 1, 2, 3$ defines the principal axes of the ellipsoid, V is the volume of the particle, ϵ_p and ϵ_s are the permittivities of the particle and of the surrounding dielectric medium, respectively, and L_m is the shape factor describing the flattening of the particle. For spherical particles the shape factor is $1/3$ for the three axes, while it deviates from this value for oblate and prolate spheroids. For the calculations presented later, we consider disk-shaped particles that have two equal principal axes defining their diameter and a shorter one defining the height of the disk. The shape factors for the particles described in this manuscript are for the long axes in the range $0.01 < L_m < 0.03$.

For scatterers of finite size, both dynamic depolarization and radiative damping influence the polarizability. In the modified long wavelength approximation, which holds for particles of subwavelength dimensions, the polarizability becomes [37]

$$\alpha_m = \frac{\alpha_m^{\text{static}}}{1 - \frac{2}{3}ik^3\alpha_m^{\text{static}} - \frac{k^2}{r}\alpha_m^{\text{static}}}, \quad (6)$$

in which $k = 2\pi\sqrt{\epsilon_s}\nu/c$ is the incident wave vector and r is half the main axis of the ellipsoid. The term $\frac{2}{3}ik^3\alpha_m^{\text{static}}$

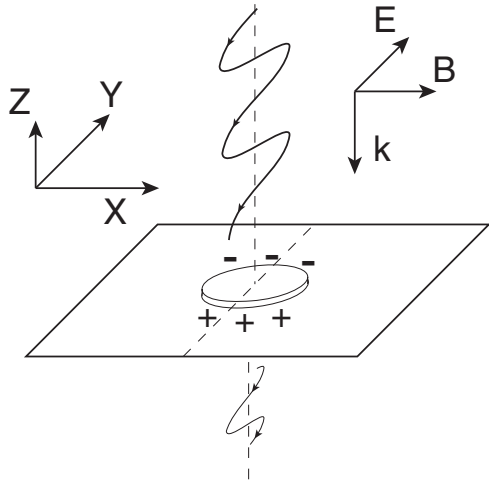


Figure 2. Schematic representation of the particle geometry and illumination.

corresponds to the dynamic depolarization, and the term $\frac{k^2}{r} \alpha_m^{\text{static}}$ to the radiative damping. The extinction cross section of the particle is determined by the amount of work done by the incident electromagnetic field on driving the charges, normalized by the intensity of the incident field. This work is given by the product of the wave vector and the imaginary component of the polarizability. When illuminated by an incident field polarized along one of the principal axes m of the particle this translates to an extinction cross section $C_{\text{ext}} = 4\pi k \text{Im}(\alpha_m)$ [37].

Calculations of the extinction cross section of GaAs micro-ellipsoids with two identical long axes of varying lengths and a short axis of $1.5 \mu\text{m}$, are shown in figure 3. This height is chosen such that the structures can be made by thin film deposition and optical lithography [35].

The incident electromagnetic field is chosen such that the wave vector is parallel with the short axis of the ellipsoid along the z-axis, and a polarization along one of the long axes of the ellipsoid in the y-direction. A scheme of the geometry is shown in figure 2. The extinction cross section is normalized against the geometrical cross section of the respective ellipsoids, resulting in the extinction efficiency Q_{ext} . The GaAs particles are considered to be surrounded by a lossless material with $\epsilon_s = 4$, representing quartz at THz frequencies. The extinction spectra are calculated for diameters $50 \mu\text{m}$ (a), $60 \mu\text{m}$ (b) and $80 \mu\text{m}$ (c), and by varying the carrier concentration in GaAs in the range 2×10^{17} to 10^{19}cm^{-3} (different curves in figure 3). All the spectra show a resonant behavior that corresponds to the coherent and resonant oscillation of the charge carriers in the particle, i.e., the LSPs in conducting GaAs.

The resonant frequency and the spectral width of the LSP are shown in figure 4, as a function of the disk diameter and carrier concentration. Due to the asymmetric shape of the LSP resonance and in order to have a clear comparison with the spectra discussed in the next section, we define the resonance width at the lower frequency half-width at half-maximum (HWHM). Increasing the particle diameter gives rise to a pronounced redshift of the LSP resonance (figure 4(a)). This redshift can be qualitatively described by

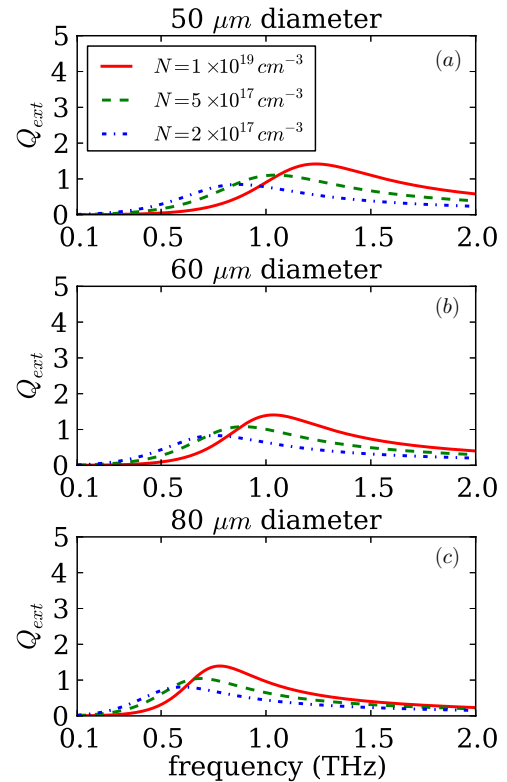


Figure 3. Extinction efficiencies of GaAs ellipsoids as a function of the size and carrier concentration under normal incidence illumination. The dash-dotted blue curves indicate a carrier concentration of $2 \times 10^{17} \text{cm}^{-3}$, the dashed green curves $5 \times 10^{17} \text{cm}^{-3}$, and the solid red curves 10^{19}cm^{-3} . Figures (a)–(c) show the extinction spectra for ellipsoids having long diameters in a plane perpendicular to the incident wave vector of $50 \mu\text{m}$, $60 \mu\text{m}$ and $80 \mu\text{m}$, respectively. All ellipsoids have a short axis parallel to the incident wave vector of $1.5 \mu\text{m}$ and are surrounded by a dielectric with a permittivity of $\epsilon_s = 4$.

the decrease in the oscillator restoring force of the charge density as the distance between charges of different sign increases. Increasing the carrier concentration increases the plasma frequency ω_p and blueshifts the resonant extinction spectrum as a consequence of the increased oscillator restoring force. We can also see that the HWHM is reduced as the particle diameter is increased (figure 4(b)). The strong dispersion of GaAs and the resonance shifts as the particle size is varied give rise to this reduction of the HWHM for larger particles: the larger values of the permittivity at lower frequencies are responsible for the reduction of the skin depth of GaAs and the concomitant reduction of the Ohmic losses, thus the narrowing of the resonance.

3. Arrays of plasmonic particles

When multiple dipolar particles are placed in close proximity, the field scattered by each of them will reach its neighbors, i.e., the neighboring particles will couple radiatively. The interference of this scattered field with the incident field can modify the overall scattering behavior of the ensemble. Diffraction becomes relevant when the particles are placed in an ordered periodic array. Diffracted orders in the plane of the

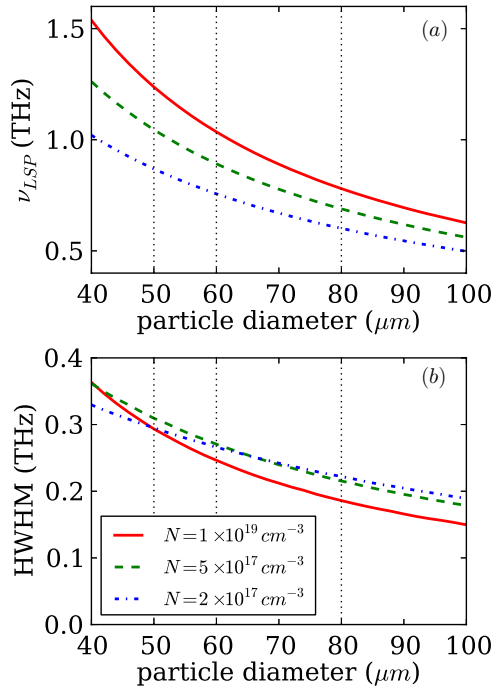


Figure 4. The LSP resonance frequency (a) and the lower frequency HWHM (b) as a function of the long axis of the ellipsoid for the different carrier concentrations. The vertical dotted lines indicate the particle diameters for the extinctions shown in figure 3.

array, known as RA, are responsible for an enhanced radiative coupling between the particles. This enhanced coupling results in hybrid diffraction-plasmonic modes known as SLRs. In this section we discuss SLRs in arrays of THz plasmonic particles and their effect on the extinction spectrum of the arrays. In order to investigate the hybridization of an LSP with a diffracted order it is important that higher orders are well separated in frequency. The simplest configuration meeting this condition is a 1D periodic lattice of scatterers.

3.1. Coupled dipole model

The polarization of each particle in an array (labeled with the subindex i) is defined as the product of its polarizability tensor with the local field at the particle position E_i^{loc} , which is the sum of the incident field, E_i^{in} , and the scattered field by all other particles, E_i^{sca}

$$p_i = \alpha_i E_i^{\text{loc}} = \alpha_i (E_i^{\text{in}} + E_i^{\text{sca}}). \quad (7)$$

The scattered field produced by a point dipole representing particle j at the position of particle i is given by the product of the dipole moment p_j and the Green's function of dipole j at the position of particle i , $G_{i,j}$. For an array of dipoles the polarization of particle i is thus given by

$$p_i = \alpha_i \left[E_i^{\text{inc}} + \sum_{j \neq i} G_{i,j} p_j \right]. \quad (8)$$

For a large array of indistinguishable particles the polarization is independent of the particle position. Only for a small fraction of particles within an interaction length of a boundary does

$P \equiv p_i = p_j$ not hold. Considering an array large enough to neglect this fraction, we can express the polarization as

$$P = \frac{\alpha E^{\text{inc}}}{1 - \alpha \sum_j G_{i,j}} = \alpha^* E^{\text{inc}}, \quad (9)$$

where the effective polarizability α^* is defined as

$$\alpha^* = \frac{1}{1/\alpha - S}. \quad (10)$$

The term $S = \sum_j G_{i,j}$ describes the coupling between the dipoles due to scattering.

When the array is illuminated such that the incident wave vector is parallel with the short axes of the ellipsoids, and the polarization direction is orthogonal to the direction of the array, we can use the scalar approximation for the polarizability and fields. Under these conditions the coupling term S for a 1D array is given by [18]

$$S = \sum_{\text{dipoles}} \exp(ikr) \left(\frac{ik}{r^2} - \frac{1}{r^3} + \frac{k^2}{r} \right), \quad (11)$$

in which r is the distance of the respective dipoles. The scalar approximation is justified since, as a result of symmetry, the polarization of the particles is always parallel with the polarization of the incident field. The extinction cross section of the coupled system in terms of this effective polarizability can now be written as

$$C_{\text{ext}} = 4\pi k \text{Im}(\alpha^*). \quad (12)$$

An interesting situation in periodic arrays occurs at the frequency at which the incident field is diffracted in the direction parallel to the array, i.e., at the RA condition. This condition can be established by the conservation of the wave vector parallel to the interface, which for a plane wave incident normal to the surface leads to $\nu = mc/(a\sqrt{\epsilon_s})$, where c is the speed of light in vacuum, m an integer defining the diffracted order and a the period of the array.

3.2. GaAs surface lattice resonances

To illustrate the diffractive coupling of LSPs in a row of identical scatterers forming a 1D periodic array we set the lattice constant to 150 μm , which results in a RA at 1 THz in a surrounding medium with $\epsilon_s = 4$. The second order RA is at 2 THz, and it is largely detuned in frequency from the first order. For scatterers with the same properties and dimensions as described in section 2.2, the extinction spectra of a row of identically coupled ellipsoidal particles are calculated and displayed in figure 5. As in figure 3, the particles have long axes of 50 μm , 60 μm and 80 μm in (a), (b) and (c), respectively, a height of 1.5 μm and are surrounded by a dielectric with permittivity $\epsilon_s = 4$, e.g., quartz. The extinction cross sections are calculated using the coupled dipole method for a 1D array of 2000 particles and normalized to the geometrical cross sections of the respective particles. For this number of particles the spectra are converged to the infinite array.

Two main and distinct features can be appreciated in the spectra of figure 5. First, at the frequency of the RA the extinction efficiency is reduced. This reduction is a

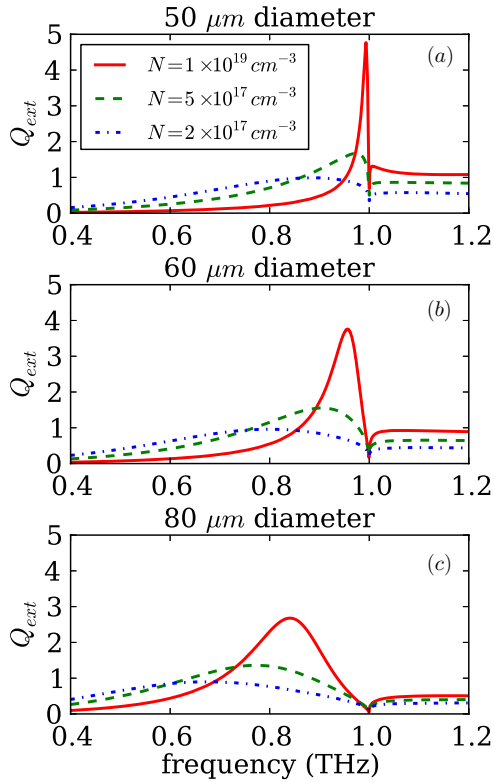


Figure 5. Extinction efficiencies of arrays of 2000 GaAs ellipsoids in a medium with permittivity $\epsilon_s = 4$ as a function of size and carrier concentration under normal incidence illumination. The pitch is $150 \mu\text{m}$, resulting in a Rayleigh anomaly at 1 THz. Figures (a), (b) and (c) show the extinction spectra for ellipsoids having diameters of $50 \mu\text{m}$, $60 \mu\text{m}$ and $80 \mu\text{m}$, respectively. All ellipsoids have a height of $1.5 \mu\text{m}$.

consequence of the scattered field from each particle being out of phase with the local incident field. Second, a pronounced resonance with an enhanced extinction appears at frequencies lower than the RA. For these frequencies the scattered field is in phase with the incident field. These resonances with enhanced extinction are known as SLRs [20] and, besides of their large extinction, they are characterized by a narrow line width. This characteristic highlights the hybrid character of SLRs originating from the enhanced radiative coupling of localized plasmonic resonances mediated by photonic/diffraction modes. The hybrid character can be also appreciated in the dependence of the resonant frequency and width with the particle size as shown in figure 6. Similar to the resonances of the individual particles shown in figure 4(a), the SLR blueshifts by decreasing the long axes of the ellipsoid and by increasing the carrier concentration. However, the blueshift in the array is limited by the frequency of the RA at 1 THz. A more remarkable difference with LSPs can be found in the dependence of the HWHM with the particle diameter. The smaller the particle diameter, the stronger the radiative coupling of the LSPs mediated by the Rayleigh anomaly, and the narrower the resonance becomes. The coupling strength is determined by the detuning between the resonant frequency of the LSPs and the RA. This characteristic makes it possible to actively control the extinction by particle arrays, enhancing

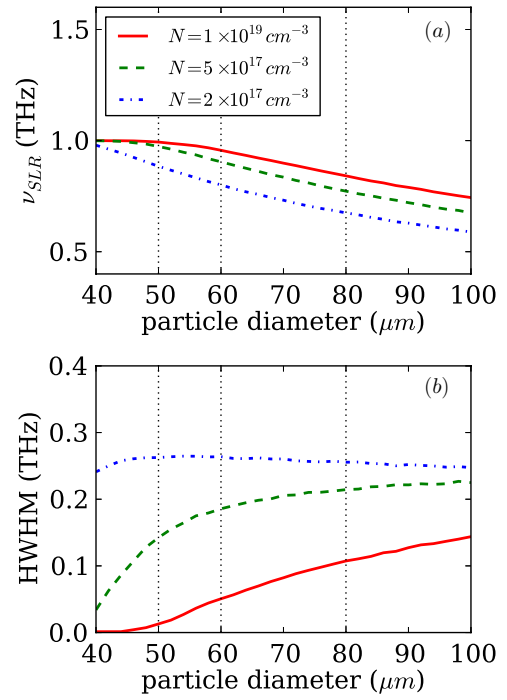


Figure 6. The SLR resonance frequency (a) and the lower frequency HWHM (b) as a function of the ellipsoid diameter for the different carrier concentrations. The dotted black vertical lines indicate the particle diameters for the curves shown in figure 5.

or suppressing it by tuning the carrier concentration in the semiconductor.

The mechanism enabling the tuneability of the extinction is further elucidated in figure 7. Figure 7(a) shows both the LSP (dashed curves) and SLR (solid curves) spectra of a disk having a diameter of $60 \mu\text{m}$ for the carrier concentrations 2×10^{17} , 5×10^{17} and 10^{19}cm^{-3} , as shown in figures 3(b) and 5(b). In figure 7(b) the real component of $1/\alpha$ for these carrier concentrations is compared against both components of S . The extinction of the coupled system has a maximum whenever the real component of $(1/\alpha - S)$ vanishes, i.e., at the poles in the real axis of the effective polarizability given in (10). The maxima in extinction are indicated by the dotted lines in figure 7(a). These lines mark also the crossing of $\text{Re}(1/\alpha)$ with $\text{Re}(S)$ at frequencies below 1 THz. The array factor S has a large value at the RA, i.e. 1 THz, as indicated by the vertical black dashed line, dominating the denominator in equation (10) and minimizing α^* . The asymptotic behavior at the RA also explains why in figure 6 the SLR frequency is limited to frequencies lower than 1 THz. By tuning the carrier concentration, and thus the magnitude of α , the frequency at which $\text{Re}(1/\alpha)$ equals $\text{Re}(S)$, thus the SLR, can be precisely controlled. We can see in figure 7(b) that $\text{Re}(1/\alpha) = \text{Re}(S)$ for a carrier concentration of $N = 10^{19} \text{cm}^{-3}$ at 1.08 THz, while for this frequency we do not observe a maximum in the extinction efficiency. The reason for the absence of this maximum is the large value of the imaginary component of S , represented by the magenta curve in figure 7(b), which reduces the extinction efficiency defined in (12).

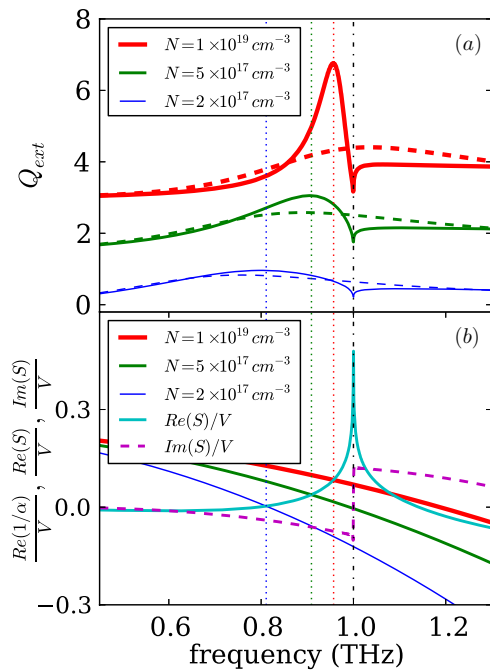


Figure 7. (a) SLRs in diffractively coupled ensembles of GaAs ellipsoids with a $60 \mu\text{m}$ diameter as shown in figure 5(b) (solid curves), and the uncoupled responses as shown in figure 3(b) (dashed curves). For clarity the spectra are displaced vertically. The real and imaginary components of the array factor S as calculated with the coupled dipole approximation for a 1D array of 2000 particles, and for each carrier concentration $1/\alpha$. The dotted lines mark the extinction maxima, and the crossings of $Re(1/\alpha)$ with $Re(S)$, the dash-dotted line marks the Rayleigh anomaly condition. S and $1/\alpha$ are normalized against the ellipsoid volume V .

4. Conclusion

We have investigated theoretically the THz extinction by individual GaAs particles and by periodic arrays. The localized surface plasmon resonance in individual particles depends on both the particle diameter and the charge carrier density. Using the coupled dipole approximation, we show that a 1D lattice of these particles can exhibit an enhanced extinction which is the result of the radiative coupling of localized surface plasmons through diffraction. The possibility to tune the resonance frequency and strength of localized plasmons by controlling the carrier density in the GaAs particles, enables control of the enhanced THz extinction in periodic arrays. This approach may be interesting for the development of efficient THz modulators.

Acknowledgments

This work is part of the research programme of the Foundation for Fundamental Research on Matter (FOM), which is part of the Netherlands Organisation for Scientific Research (NWO). The authors thank Audrey Berrier for fruitful discussions. JGR acknowledges financial support of the European Research Council through the ERC-stg 259272 THz PLASMON.

References

- [1] Bharadwaj P, Deutsch B and Novotny L 2009 Optical antennas *Adv. Opt. Photon.* **1** 438–83
- [2] Giannini V, Fernandez-Dominguez A I, Heck S C and Maier S A 2011 Plasmonic nanoantennas: fundamentals and their use in controlling the radiative properties of nanoemitters *Chem. Rev.* **111** 3888–912
- [3] Ebbesen T W, Lezec H J, Ghaemi H F, Thio T and Wolff P A 1998 *Nature* **391** 667
- [4] Gómez Rivas J, Schotsch C, Haring Bolivar P and Kurz H 2003 Enhanced transmission of THz radiation through subwavelength holes *Phys. Rev. B* **68** 201306
- [5] Gómez Rivas J, Kuttge M, Haring Bolivar P, Kurz H and Sánchez-Gil J A 2004 Propagation of surface plasmon polaritons on semiconductor gratings *Phys. Rev. Lett.* **93** 256804
- [6] Han J, Lakhtakia A, Tian Z, Lu X and Zhang W 2009 Magnetic and magnetothermal tunabilities of subwavelength-hole arrays in a semiconductor sheet *Opt. Lett.* **34** 1465–7
- [7] Yin H and Hui P M 2009 Controlling enhanced transmission through semiconductor gratings with subwavelength slits by a magnetic field *Appl. Phys. Lett.* **95** 011115
- [8] Gómez Rivas J, Kuttge M, Kurz H, Haring-Bolivar P and Sánchez-Gil J A 2006 Low-frequency active surface plasmon optics on semiconductors *Appl. Phys. Lett.* **88** 082106
- [9] Sánchez-Gil J A and Gómez Rivas J 2006 Thermal switching of the scattering coefficients of terahertz surface plasmon polaritons impinging on a finite array of subwavelength grooves on semiconductor surfaces *Phys. Rev. B* **73** 205410
- [10] Chen M-K, Chang Y-C, Yang C-E, Guo Y, Mazurowski J, Yin S, Ruffin P, Brantley C, Edwards E and Luo C 2010 Tunable terahertz plasmonic lenses based on semiconductor microslits *Microw. Opt. Technol. Lett.* **52** 979–81
- [11] Janke C, Gómez Rivas J, Haring-Bolivar P and Kurz H 2005 All-optical switching of the transmission of electromagnetic radiation through subwavelength apertures *Opt. Lett.* **30** 2357–9
- [12] Gómez Rivas J, Sánchez-Gil J A, Haring-Bolivar P and Kurz H 2006 Optically switchable mirrors for surface plasmon polaritons propagating on semiconductor surfaces *Phys. Rev. B* **74** 245324
- [13] Hendry E, Garcia-Vidal F J, Martin-Moreno L, Gómez Rivas J, Bonn M, Hibbins A P and Lockyear M J 2008 Optical control over surface plasmon polariton-assisted THz transmission through a slit aperture *Phys. Rev. Lett.* **100** 12390
- [14] Azad A K *et al* 2009 Ultrafast optical control of terahertz surface plasmons in subwavelength hole arrays at room temperature *Appl. Phys. Lett.* **95** 011105
- [15] Okada T, Tsuji S, Tanaka K, Hirao K and Tanaka K 2010 Transmission properties of surface plasmon polaritons and localized resonance in semiconductor hole arrays *Appl. Phys. Lett.* **97** 261111
- [16] Chen H-T, Lu H, Azad A K, Averitt R D, Gossard A C, Trugman S A, O'Hara J F and Taylor A J 2008 Electronic control of extraordinary terahertz transmission through subwavelength metal hole arrays *Opt. Express* **16** 7641
- [17] Zou S, Janel N and Schatz G C 2004 Silver nanoparticle array structures that produce remarkably narrow plasmon lineshapes *J. Phys. Chem. B* **120** 10871
- [18] Zou S and Schatz G C 2004 Narrow plasmonic/photonic extinction and scattering line shapes for one and two dimensional silver nanoparticle arrays *J. Chem. Phys.* **121** 12606
- [19] Hicks E M, Zou S, Schatz G C, Spears K G, VanDuyne R P, Gunnarsson L, Rindzevicius T, Kasemo B and Käll M 2005

- Controlling plasmon line shapes through diffractive coupling in linear arrays of cylindrical nanoparticles fabricated by electron beam lithography *Nano Lett.* **5** 1065–70
- [20] García de Abajo F J 2007 Light scattering by particle and hole arrays *Rev. Mod. Phys.* **79** 1267
- [21] Kravets V G, Schedin F and Grigorenko A N 2008 Extremely narrow plasmon resonances based on diffraction coupling of localized plasmons in arrays of metallic nanoparticles *Phys. Rev. Lett.* **101** 87403
- [22] Auguie B and Barnes W L 2008 Collective resonances in gold nanoparticle arrays *Phys. Rev. Lett.* **101** 143902
- [23] Chu Y, Schonbrun E, Yang T and Crozier K B 2008 Experimental observation of narrow surface plasmon resonances in gold nanoparticle arrays *Appl. Phys. Lett.* **93** 181108
- [24] Vecchi G, Giannini V and Gomez Rivas J 2009 Shaping the fluorescent emission by lattice resonances in plasmonic crystals of nanoantennas *Phys. Rev. Lett.* **102** 146807
- [25] Giannini V, Vecchi G and Gómez Rivas J 2010 Lighting up multipolar surface plasmon polaritons by collective resonances in arrays of nanoantennas *Phys. Rev. Lett.* **105** 266801
- [26] Zhou W and Odom T W 2011 Tunable subradiant lattice plasmons by out-of-plane dipolar interactions *Nature Nanotechnol.* **6** 423–7
- [27] Bitzer A, Wallauer J, Helm H, Merbold H, Feurer T and Walther M 2009 Lattice modes mediate radiative coupling in metamaterial arrays *Opt. Express* **17** 22108–113
- [28] Ng B, Hanham S M, Giannini V, Chen Z C, Tang M, Liew Y F, Klein N, Hong M H and Maier S A 2011 Lattice resonances in antenna arrays for liquid sensing in the terahertz regime *Opt. Express* **19** 14653–61
- [29] Singh R, Rockstuhl C and Zhang W 2010 Strong influence of packing density in terahertz metamaterials *Appl. Phys. Lett.* **97** 241108
- [30] Wallauer J, Bitzer A, Waselikowski S and Walther M 2011 Near-field signature of electromagnetic coupling in metamaterial arrays : a terahertz microscopy study *Opt. Express* **19** 3212–17
- [31] Grant J, Shi X, Alton J and Cumming D R S 2011 Terahertz localized surface plasmon resonance of periodic silicon microring arrays *J. Appl. Phys.* **109** 054903
- [32] Ashcroft N W and Mermin N D 1976 *Solid State Phys.* (London: Brooks/Cole)
- [33] Hilsun C 1974 Simple empirical relationship between mobility and carrier concentration *Electron. Lett.* **10** 259–60
- [34] Adachi S 2004 *Handbook on Physical Properties of Semiconductors* vol 1–3 (Berlin: Springer)
- [35] Berrier A, Ulbricht R, Bonn M and Gomez Rivas J 2010 Ultrafast active control of localized surface plasmon resonances in silicon bowtie antennas *Opt. Express* **18** 23226–35
- [36] Van de Hulst J C 1981 *Light Scattering by Small Particles* (New York: Dover)
- [37] Jensen T, Kelly L, Lazarides A and Schatz G C 1999 Electrostatics of noble metal nanoparticles and nanoparticle clusters *J. Cluster Sci.* **10** 295